Ročník 2011 electroscope Číslo II

Impact of Local Defects on Photon Emission, Electric Current Fluctuation and Reliability of Silicon Solar Cells Studied by Electro-Optical Methods

R. Macku[1], P. Koktavy[1]
[1] Department of Physics, Faculty of Electrical Engineering and Communication, Brno University of Technology
Technicka 8, 616 00 Brno, Czech Republic
E-mail : robert.macku@phd.feec.vutbr.cz, koktavy@feec.vutbr.cz

Abstract:
This paper, for the first time, investigates localized defects of silicon solar cells. These imperfections represent real problem because of solar cell long-term degradation and decreasing conversion efficiency. To solve this issue, this paper does systematic research about optical investigation of local defect spots and correlation with rectangular microplasma fluctuation. Sensitive CCD camera has been used for mapping of surface photon emission. The operation point of the samples has been set to reverse bias mode and the different electric field intensity was applied. It turns out, that some solar cells exhibit an imperfection in the bulk and close to the edges. Nevertheless, we confine ourselves to bulk defects of potential barrier. We managed to get interesting information using combination of optical investigations and electrical noise measurement in the time and spectral domain. It will be revealed that a direct correlation between noise and photon emission exists and the results related to several defect spots are presented in detail in this paper.

INTRODUCTION

The mechanism of reverse-biased junction conductivity appears to be due to crystalline lattice imperfections, dislocations, or metallic precipitates in the *pn* junction region. Local breakdowns will thus take place in the neighbourhood of such a defect at reverse voltages below those required for a breakdown in a defect-free region of the junction.

Diagnostics of defect areas can be carried out by one or several of the following methods: scanning the time response of the reverse current, measurement of VA characteristics, measurement of RMS value of narrowband current noise at reverse current or voltage, measurement of noise power spectral density, measurement of the radiation emitted from the defect during micro-plasma discharge formation. The latter method is applicable to optoelectronic devices and solar cells and it will be mainly presented in this paper.

Practical motivation for defect inspection, expected conversion efficiency, is situation when a certain part of the cell operating in a solar panel happens to be in a local shade, this particular cell will get into reverse-bias condition. Due to the existence of reduced breakdown voltage local defects, local breakdowns may occur in the neighbourhood of the defects, which in turn may lead to heavy current densities in the low-cross-section regions. This phenomenon can give rise to a heavy local temperature increase and, consequently, local diffusion or thermal breakdown, which may result in the cell destruction.

From physical point of view, three fundamental types of local defects can be observed. The existence of the first one is accompanied by local avalanche breakdowns in cells polarized in reverse direction. It evokes microplasma noise waveform in a form of random rectangular impulses in an external circuit with noise power spectral density of generation-recombination type. The second type can be caused by Zener breakdown. The third type is determined by the existence of conductive channels where flowing current evokes local lattice heating and it can lead to thermal breakdown of local regions in *pn* junctions in reverse direction. The current noise power spectral density is in a form of $1/f$ noise for this case.

All types of these processes can give rise to weak local emission of light from reverse biased *pn* junction local regions and we can observe light spots on the surface on solar cells, see Fig. 3, 4, 5. This visible radiation can be emitted from silicon reverse-biased *pn* junction by direct transitions due to hot carriers which are present during avalanche or Zener breakdowns, [1], for the first and second mentioned case. The spectral distribution of the avalanche breakdown radiation is known to be continuous from 1.1 eV up to 3.3 eV, [2]. Radiation in the third case is caused due to local lattice heating and it is determined by Planck's law. Since radiation sources are placed very near the centre of the *pn* junction, observed radiation from a solar cells surface can be affected by absorption in the surrounding silicon.

SAMPLES DETAIL

In the broader context, we carried out experiments with two types of the solar cells. One of them has a traditional pyramidal texture and other has so-called "table" texture. Thanks to an appropriate texture, multiple reflections and better radiation absorption are achieved. Moreover, table textured solar cells are

optimized for absorption of the infrared radiation and they are left out of consideration here. Figure 1 shows the texture of studied solar cells. Topography image has been obtained by the SNOM (scanning near-field optical microscope) microscope. The *pn* junction is localized close to the surface and traces pyramidal texturization. The depletion layer width is about of 0.6 μm (without the applied bias voltage).

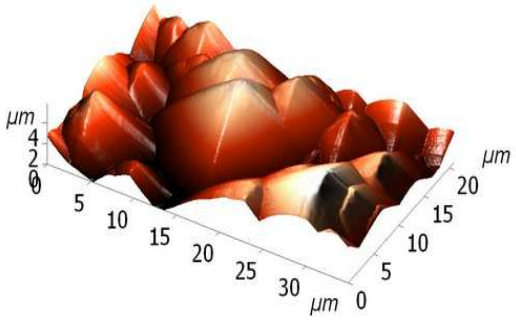

Fig. 1: The solar cell surface topography image, SNOM, Velocity = 12.03 μm/s, Setpnt = 3.9 V

Primary parameters of the samples follow. The solar cells are made from single-crystal silicon, of dimensions 12×12 cm and a thickness of 230 μm. The *p* and *n* (bottom and top-side, respectively) layers are formed by diffusion. The *p* type substrate is made by the Czochralsky process with the resistivity of about 1.2 Ωcm. A silicon nitride layer, which is laid on the cell surface, is intended to passivate the silicon surface and also reduces the reflection losses. The cells are designed for the solar panel fabrication. Both complete cells and their broken fragments have been studied but only selected results are presented here. The screen-printed silver paste metallization was used for contacts on the front side. The back side of solar cells has a structure of Al BSF with Ag/Al busbars.

EXPERIMENTAL SET-UP

Radiation generated from reverse-biased *pn* junction defects is used to study local properties (far field detection). It proves to be useful to measure surface radiation and to make light spots localization, to measure the radiation intensity versus voltage plot, its correlation with other, mainly noise characteristics and radiation spectrum.

A scientific CCD camera G2-3200 with a 3.2 MPx resolution was used for measuring of the radiation from a *pn* junction solar cell surface. It uses a silicon chip cooled by dual system of Peltier's modules with the operation temperature down to -50 °C. The sufficient temperature for normal working mode is of -10 °C. The Dark current of an optical sensor and a single pixel is 0.8 e/s (it holds for T = 0 °C) and the doubling of its value is reached for a temperature rise of 6 ° C. The dynamic range of the elementary pixels with a usable range up to 16 bits is very good. A camera lens with focal ratio 1.2 and working aperture 41.7 mm is used with the camera. It is possible to measure in the useful range of wavelengths of 300 nm – 1100 nm. Since the producer defines the spectral characteristics of the particular CCD chip, photometry measurements can be performed as in our case. The mean quantum efficiency <QE> = 0.51 is reached in the interval 300 - 1100 nm. The peak value of the quantum efficiency is of 0.82 at a wavelength of 647 nm. Optical filters are included to an optical path to obtain the spectral characteristics. FWHM (Full Width at Half Maximum) of the regular filters are 150 nm and their optical response is calibrated. It is possible to include interference filters with FWHM of about 10 nm ahead of the lens. Detected radiation is relatively weak due to their high selectivity and this measurement is very technically and time demanding. The calibration is not performed separately for each of these filters, but measurement is carried out with the average spectral transmission function. The results are therefore correct in principle but we work with them in relative terms.

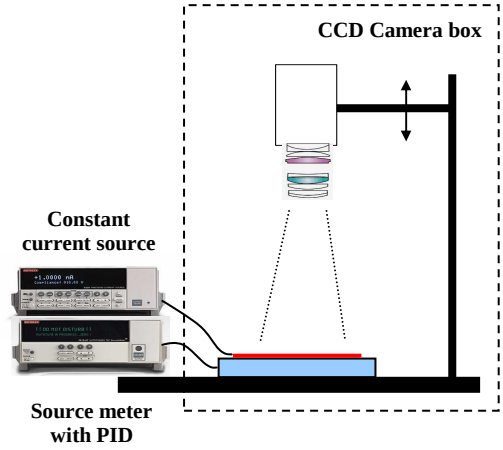

Fig. 2: Schematic illustration of experimental set-up

The CCD Camera along with the solar cell sample is in the optically shielded chamber (see Fig. 2). The sample temperature is kept constant during measurement by the PID temperature regulator integrated in Keithley source meter. Sample bias is realized by constant current source controlled via IEEE 488.2 bus.

OPTICAL CHARACTERIZATION

Figure 3 depicts fragment of the solar cell K20 with five spots emitting light. It should be emphasized here that the photon emission intensity of the light spots depends on the applied voltage and some of them are suddenly activated with the increasing DC electric field. Figure 3 represents high contrast photography of solar cell dual exposition in the dark and with bias light. There are labelled observable defect spots with different optical and electrical character. We managed to achieve good edge isolation and leakage current may be neglected here.

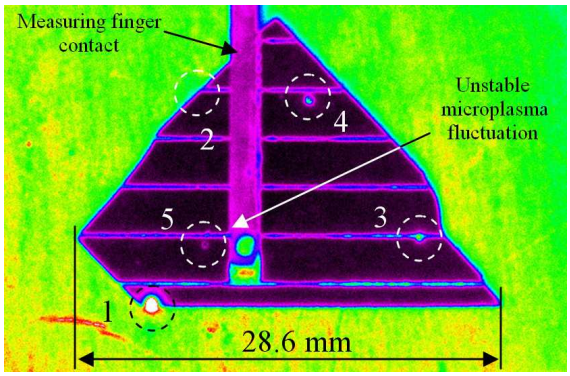

Fig. 3: Photography of measured solar cell with light spots, sample K20, reverse voltage 10 V

Light spots represents, in general, local fluctuations of the *pn* junction width and potential barrier width. It leads to decreasing of the breakdown voltage and local breakdown (conductive channels) may be created, [2], [3]. Local conductive channels concentrate curret from neighbourhood and heavy current densities effects on low dimension region. This phenomenon can give rise to a heavy local temperature increase and, consequently, local diffusion or thermal breakdown, which may result in the solar cell destruction.

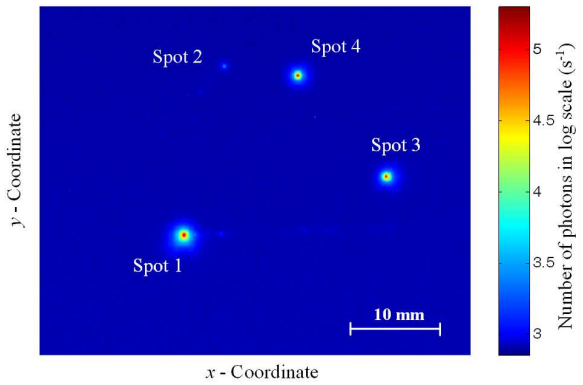

Fig. 4: Light spots and their intensity before avalanche breakdown in spot 5, sample K20, reverse voltage 9 V

Three essential types of defect can be observed as a result of potential barrier fluctuation. First of all let's pay attention to local avalanche breakdowns. If electric field intensity is high enough, act of impact ionization followed by avalanche multiplication occurs. It evokes the microplasma noise waveform in a form of random rectangular impulses (see Fig. 9) in an external circuit with the noise power spectral density of generation-recombination type (see Fig. 10), [3], [4]. It should be noted here, that avalanche breakdowns may not necessarily generate current fluctuations. The second mechanism is tunneling through a potential barrier. Last but not least the flowing current can give rise to thermal astabilities. Consider localized regions in a semiconductor material where conductivity is higher compare to neighbouhood. Naturally the current will flow above all through these regions. Power dissipation increases along with conductivity. Consequently local lattice heating leads to thermal astabilities and breakdown.

The first light (see spot 1, Fig. 4) was detected at the sample edge for the reverse voltage from about 4 V. We suppose that the light generation for this case do not evoke by avalanche breakdown with respect to low value of the reverse voltage and the detection limit of CCD camera. It is clear from electrical measurements that the last light spot (spot 5) relates with microplasma noise (Fig. 4, Fig. 5) and it is caused by local avalanche breakdown. Light generation from this spot starts from the reverse voltage of 9.7 V. The solar cell with light spots before and after avalanche breakdown in the spot 5 is in Fig. 4 and Fig. 5.

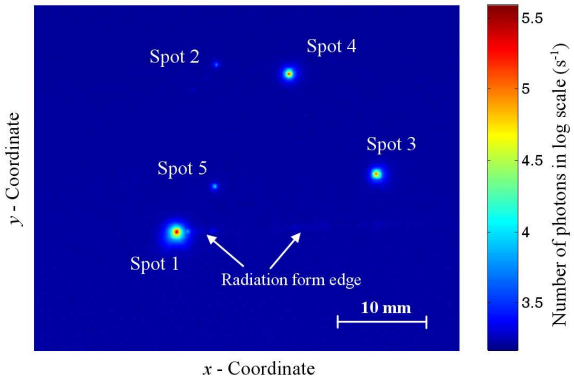

Fig. 5: Edge radiation and light spots with their intensity after avalanche breakdown in spot 5, sample K20, reverse voltage 10 V

In addition, photon emission, in wavelength range 300 nm - 1100 nm, expressed in number of photons per second versus reverse voltage was measured. Results for individual light spots, presented before, are depicted in Fig. 6.

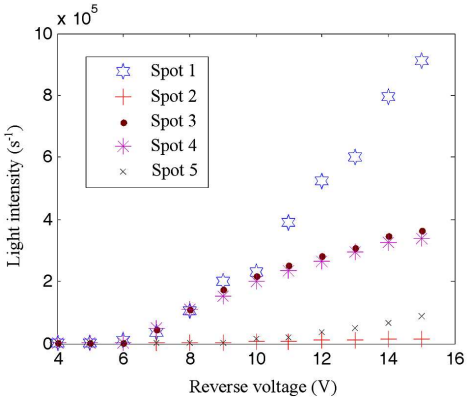

Fig. 6: Intensity of radiation in number of photons per second versus reverse voltage, wavelength interval 300 nm to 1100 nm, sample K20

Light intensity has been measured in the center of light spots as their maximum. It is clear, that curvature and slope is different and light spots have a different character. Further information is possible to obtain from optical spectrum measurement. Figure 8 depicts optical spectrum again for individual light

spots. It should be noted here, that spot 2 was excluded from measurement because of weak radiation intensity.

Measurement has been done using accurate interference filters included into optical path. Optical filters properties (FWHM and insertion loss) weakly fluctuate with the center wavelength. On this account results are presented in relative units and as a reference point was choose the spot 1 at 1100 nm. An interesting fact is that although at least the spots 1 and 5 have probably different nature, optical spectrum of all light spots is very similar. The depth of the *pn* junction centre is about 70 nm for our samples of solar cells. It means that the source of light emission in the *pn* junction must be placed about 70 nm below the cell surface. Absorption coefficient, α, of the silicon is approximately $(1 \div 10^4)$ cm^{-1} at room temperature and operating wavelength range. That is why we suppose that we measure an original spectrum of light without distortion by silicon.

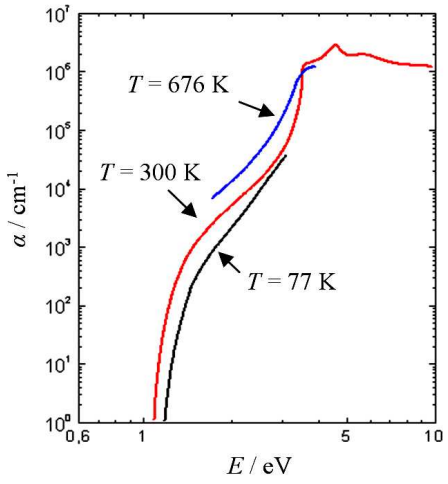

Fig. 7: The absorption coefficient of silicon vs. photon energy at different temperatures, adapted from [5].

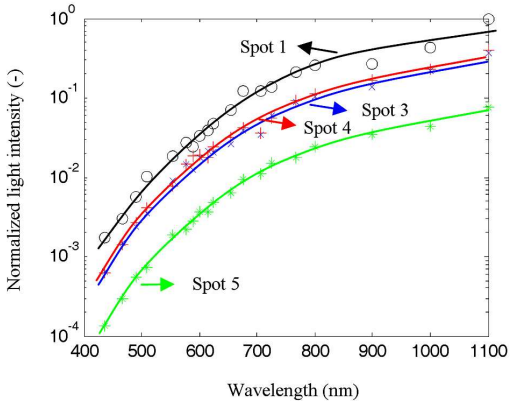

Fig. 8: Normalized light intensity versus wavelength, FWHM is about 10 nm, reference value at 1100 nm and spot 1, sample K20, reverse voltage 13.4 V

The theoretical photon spectrum emitted by a silicon solar cell is schematically shown in Fig. 9. The light intensity in relative units for each process enables form comparison. The peak at the wavelength of 1100 nm represents band-to-band luminescence process. It is emitted during a radiative recombination event of an electron and hole. Although silicon has indirect bund structure it is the most probable process. The second peak located at 1400 nm is generated by radiation via traps assisted recombination (impurities and mechanical defects). In the same picture black body radiation according the Planck's law is illustrated. All of these mechanisms are out of the CCD chip detection range in the spectral domain. What we measure is breakdown radiation due to impact ionization and avalanche multiplication. In this case, electrons are accelerated by electric field from *p* to *n* type semiconductor. Local regions become conductive in the reverse direction. The electron kinetic energy or the velocity has broad statistic distribution. On this account, inter-band recombination forms broad photon emission. The avalanche current typically decreases with the increasing temperature because of the limiting kinetic energy by collisions with the crystal lattice. Collisions are more likely because of increased thermal movement of the lattice. So, thermal dependence of radiation spectrum can be used for confirming of our assumption.

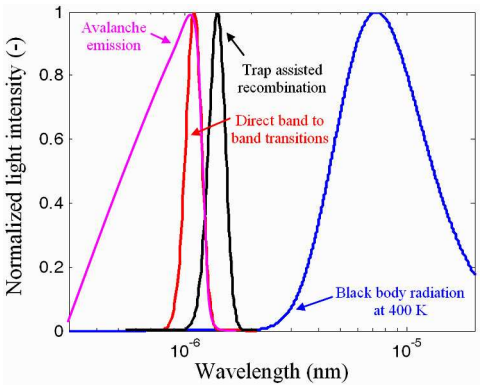

Fig. 9: Spectral characteristic of different radiative transitions - schematic illustration

NOISE SOURCES IN SOLAR CELLS

The noise diagnostics is based on the assumption that the device structure defects give rise to excess noise. As mentioned earlier we can observe number of different noise sources and their superposition respectively. In many cases the stationarity is in question and physical nature is not evident. In addition, noise developed its character with applied DC voltage, see [3], [4]. The noise experimental method has been put into connection with optical surface observation and photon emission detection. Thanks to that, we are able to distinguish the defect contributions from each other even in the case the device contains a number of field activated defects [1], [3].

The first noise type, so-called microplasma noise, usually appears at sufficiently high reverse voltages, yet lower than the breakdown voltage of the complete defect-free junction regions. It is caused by avalanche ionization breakdown in astable form, more in [3]. Figure 10 depicts microplasma current noise in the time domain.

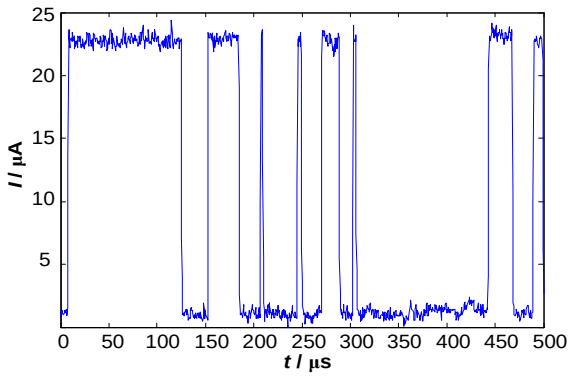

Fig. 10: Microplasma noise waveform, sample K20, reverse voltage 9.81 V

Spectral analyses show that the current noise power spectral density, which depends on the reverse voltage, is in a form of generation-recombination noise for the microplasma noise source, see Fig. 11. Since other local inhomogeneties in a *pn* junction of the presenting sample do not exhibit strong voltage dependence behaviour, it is not possible to distinguish particular noise sources. The current noise power spectral density is in a form of 1/*f* noise for the reverse voltage out from the microplasma instability region and pointed out rather thermal astable mechanism. It corresponds to non-field activated process (spot 1) as presented before. Then 1/*f* fluctuations may mask another noise sources.

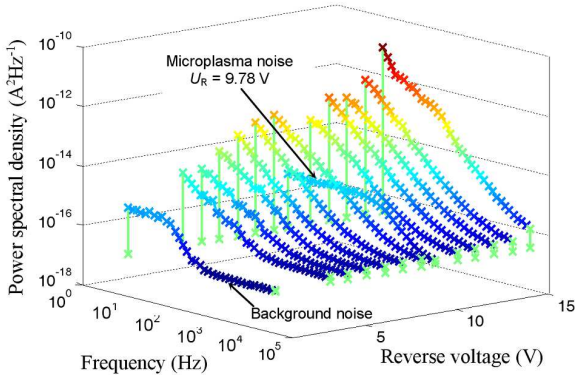

Fig. 11: Current noise power spectral density for various reverse voltages, sample K20

Note that the avalanche multiplication (or impact ionization) has a positive temperature coefficient for breakdown. Due to this fact, avalanche multiplication (or microplasma noise) we may discriminate from e.g. tunneling effect or thermal instability. Due to the fact that breakdown is a function of temperature it is necessary the temperature of the solar cell sample keep constant during measurement.

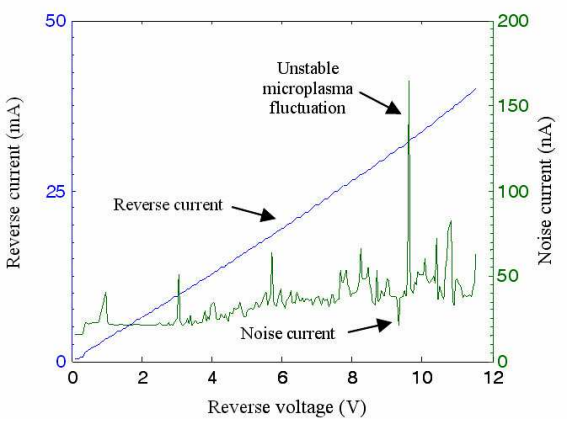

Fig. 12: Narrowband noise signal and DC current for various reverse voltages, sample K20, T = 28°C.

For purposes of non-destructive testing in production industry or/and if we want number of microplasma regions known, it is not necessary complicated PSD measurement make. The aforementioned experimental results indicate that gereration-recombination spectrum has not neglectable power in frequency region where others noises are neglectable. This effect consecutively leads to the other measurement philosophy. We can measure narrowband noise signal on the center frequency e.g. 1 kHz (see Fig. 12). We use the selective nanovoltmeter with high selectivity and effective bandwidth of about 30 Hz (effective bandwidth is sometime called noise bandwidth). The effective value of narrowband signal is measured via the DC voltmeter. Figure 12 depicts this experimentally obtained narrowband signal. It is interesting to see that microplasma regions are very close bounded and smaller peaks indicate another type of noise presence. Here was chosen center frequency 420 Hz.

CONCLUSIONS

We can conclude that electrical noise measurement, e. g. measurement of the current flowing through solar cells and its spectrum, effective narrowband values and time evolution, is very sensitive to detect defects that exhibit unstable local avalanche breakdowns and produce microplasma noise. Bulk phenomena usually produces shot current noise or 1 / *f* current fluctuations. Many defects exhibit radiation from a surface of solar cells. It proves to be useful to measure this radiation by means of the CCD camera especially for localized spots. We can make light spots localization, measure the radiation intensity versus voltage plot, its correlation with other, mainly noise characteristics and measure radiation spectrum. Next step in our research will be thermal characterization of field activated defects and temperature dependence of light radiation. It turns out that the number of light spots on the surface of solar

cells is much higher than the number of light spots caused by unstable local avalanche breakdowns. Since measured spectrum of emitted light is very similar for more types of light spots it is necessary to find additional methods for physical interpretation. Measurement of the thermal characteristics is very promising approach.

ACKNOWLEDGMENT

This paper is based on the research supported by the Grant Agency of the Czech Republic within the framework of the project P102/10/2013 "Fluctuation processes in PN junctions of solar cells" and the research intention MSM 0021630503 "New Trends in Microelectronic Systems and Nanotechnologies".

REFERENCES

[1] CHYNOWETH, A. G., McKAY, K.G. Photon Emission from Avalanche Breakdown in Silicon. *Phys. Rev*, 1956, vol. 102, no. 2, p. 369 – 376.

[2] BISHOP, J. W. Microplasma Breakdown and Hot-spots in Silicon Solar-Cells. *Solar Cells*, 1989, vol. 26, no. 4, p. 335-349.

[3] KOKTAVÝ P., MACKŮ R., PARAČKA P., KRČÁL O., Microplasma noise as a tool for PN junctions diagnostics, *WSEAS Transactions on Electronics.* 2008, vol. 4, p. 186–191.

[4] MACKŮ, R.; KOKTAVÝ, P. Analysis of fluctuation processes in forward-biased solar cells using noise spectroscopy. Physica status solidi (a). 2010. 207(10). p. 2387 - 2394. ISSN\~1862-6319.

[5] Sze S. M., Physics of Semiconductor Devices, *John Wiley & Sons, New York*, November 2006, ISBN 978-0-471-14323-9.